CAV2021
11th International Symposium on Cavitation
May 10-13, 2021, Daejon, Korea

Numerical simulation of supercavitating flow around a submerged projectile near a free surface

Van-Tu Nguyen*, Thanh-Hoang Phan, Trong-Nguyen Duy, and Warn-Gyu Park*

School of Mechanical Engineering, Pusan National University, Busan, Korea

Abstract: In this work, the flow structure of supercavitation around a submerged projectile beneath a free surface is investigated in detail using computational fluid dynamics. The supercavitating flow near the free surface is complicated by projectiles moving at high speeds and three phases including air, liquid, and vapor due to evaporation. The dual-time preconditioned Navier-Stokes (NS) model for three-phase flow is solved in a generally curvilinear structured grid by using an implicit difference discretization method based on a MUSCL/Godunov-type finite volume scheme. A compressive limiter is used to obtain sharp interfaces between the immiscible fluids. The numerical method was validated by computing a cavitating flow around a blunt cylinder body at different cavitation numbers and the numerical results are match well with available experimental data. Besides, supercaviating flow around a high-speed projectile beneath the free surface was computed and comparisons of the growth of the cavity between numerical and experimental images were presented. Subsequently, the flow of the projectile at different velocities and different depths were analyzed, through which the physical picture of this flow is clearly observed

Keywords: Cavitation; Three-phase flow; Supercavitation; Near free surface**;** High-speed

1. Introduction

Cavitation often occurs around submerged vehicles moving at a high speed. Most of the vehicles operate near a free surface and the cavitating flow around the vehicles is complicated by the presence of the free surface. Although the cavitation flow has been studied for a long time ago, the detail inside and the growth process of the cavity in many conditions still need to consolidate. Recently, the development of hydrodynamic loading on ships, missile projectile impact upon water entry, torpedo launching, ditching of aircraft, sea-landing of aerial vehicles, the motion of watercraft, and development of oceanographic measuring devices have been becoming an intensive demand. The design and control of vehicles and devices are the heart of engineering and require the synthesis of fundamental and applied scientific research for engineering decisions. Many studies regarding the flows near the free surface in the very early stages to obtain a detailed understanding of the flow [1-3]. Several studies of a projectile parallel to a free surface were also addressed using both experimental and numerical approaches [4, 5]. In the present work, we focus on the growth process of a supercaviating flow around a projectile near a free surface at various conditions and provide a physical picture of this flow. The rest of the paper is organized in the following sections: the brief numerical procedure, the validation and results, and a conclusion.

2. Numerical method

Here, the homogeneous mixture model for an incompressible three-species fluid flow is used to perform simulations in this study. The governing equations are the mixture continuity equation, the mixture momentum equations, and the phasic volume fraction equations. The mass transfer is considered to model cavitation around projectiles. Pseudo-time terms are added to the governing equations to build a dual time-stepping algorithm for unsteady computation and expressed as follows [6]:

* Corresponding Author: Van-Tu Nguyen, nguyenvantu@live.com; Warn-Gyu Park, wgpark@pusan.ac.kr

$$\frac{1}{\beta\rho^{\gamma}}\frac{\partial p}{\partial \tau}+\nabla\cdot\mathbf{u}=\dot{m}\left(\frac{1}{\rho_l}-\frac{1}{\rho_{\mathrm{v}}}\right), \quad (1)$$

$$\frac{\partial}{\partial \tau}(\rho\mathbf{u})+\frac{\partial}{\partial t}(\rho\mathbf{u})+\nabla\cdot(\rho\mathbf{u}\mathbf{u}+p\mathbf{I})=\nabla\cdot\left(\mu(\Delta\mathbf{u}+\Delta\mathbf{u}^{T})\right)+\rho\mathbf{g}, \quad (2)$$

$$\frac{\partial \alpha_l}{\partial \tau}+\left(\frac{\alpha_l}{\beta\rho^{\gamma}}\right)\frac{\partial p}{\partial \tau}+\frac{\partial \alpha_l}{\partial t}+\nabla\cdot(\mathbf{u}\alpha_l)=\frac{\dot{m}}{\rho_l}, \quad (3)$$

$$\frac{\partial \alpha_{\mathrm{v}}}{\partial \tau}+\left(\frac{\alpha_{\mathrm{v}}}{\beta\rho^{\gamma}}\right)\frac{\partial p}{\partial \tau}+\frac{\partial \alpha_{\mathrm{v}}}{\partial t}+\nabla\cdot(\mathbf{u}\alpha_{\mathrm{v}})=0, \quad (4)$$

where β is the preconditioning compressibility parameter, p is the pressure, t is the physical time, τ is the pseudo time, $\mathbf{u}$ is the flow velocity vector, α_i is the volume fraction of the i^{th} phasic component and the subscripts l, v, and $\mathbf{g}$ denote liquid, vapor, and non-condensable gas fluids, respectively. The source term of the mass transfer rate is $\dot{m}=\dot{m}^{+}+\dot{m}^{-}$, where $\dot{m}^{+}$ is the mass rate of vapor generation, and $\dot{m}^{-}$ is the mass rate of condensation [7].

3. Results and discussion

In this section, validation of cavitation flow over a blunt cylinder and supercavitating flow around a projectile beneath a free surface is presented. The simulated results are compared with available experimental data and other numerical methods. The effects of depth and velocity on the supercavitation profiles around the projectile near a free surface were investigated

3.1. Validation

To validate the numerical setup, a computation of the cavitation flow over hemispherical and blunt cylinders at a cavitation number of σ = 0.3 was performed. A grid size of 393,450 grid points was used. A nominal density ratio of 1000 is assigned for the simulations. The time-steps are restricted by the CFL conditions to a value of 0.5. Fig. 1 shows 2D and 3D cavitation profiles with streamline and pressure distribution around the body, and pressure coefficient distributions over the surface of a blunt cylinder. A good agreement of this simulation with other studies published in the literature is obtained. The numerical solutions of the surface pressures are close to experimental data and other published results, showing the reliability of the numerical procedure for simulating the growth of the cavitating flows.

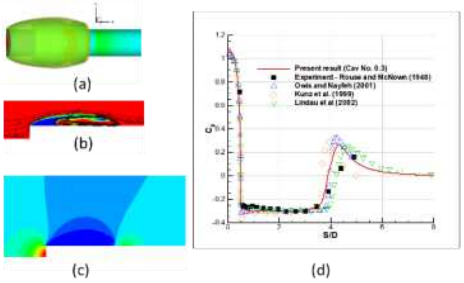

Fig. 1. Cavitation flow over a blunt cylinder at cavitation number σ = 0.3 at steady state: (a) 3D results of cavitation profile at an iso-surface of 0.5 and pressure distribution on the body surface; (b) Cavitation flow and streamline; (c) pressure distribution around the body; (d) comparison of surface pressure distributions between present results with available experiment and other predictions.

3.2. Supercaviation around a projectile beneath a free surface

This section presents a numerical investigation of supercavitating flows around a high-speed projectile near a free surface at different depths and velocities. The projectile diameter D is equal to 37 mm and it is set parallel with the free surface. The initial conditions of the five simulations are listed in Table 1. In case

* Corresponding Author: Van-Tu Nguyen, nguyenvantu@live.com; Warn-Gyu Park, wgpark@pusan.ac.kr

1, the cavitation growth process around a projectile when the upper side of the projectile coincides with the free surface was simulated at a velocity of 19.1 m/s. In other words, the submerged depth which is the distance from the free surface to the axis of the projectile is 0.5*D*. Fig.2 shows the grid refinement with a medium grid of 390,450 grid points and a refined grid of 1,355,900 grid points. The main feature of cavitation profiles between the grids are similar, only the water layer in the very upper region was not captured well by the medium grid. The figure shows that this region has a small effect on the growth of the cavitation process in this case. However, for more detailed analyses of the flow in other cases in this section, the refined grid was used.

Table 1. Description of simulation cases including initial velocity and submerged depth of the projectile.

Cases	1	2	3	4	5
Velocity (m/s)	19.1	19.1	30	40	50
Submerged depth, *H*	0.5*D*	*D*	0.5*D*	0.5*D*	0.5*D*

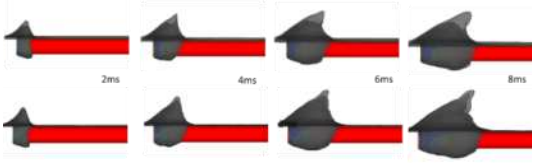

Fig. 2. Grid refinement study of supercavitating flows around underwater projectile near the free surface at velocity 19.1 m/s. Medium grid (top row) and refined grid (bottom row).

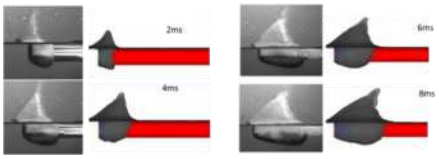

Fig. 3. Comparison of supercavitating flows around underwater projectile near the free surface at velocity 19.1 m/s.

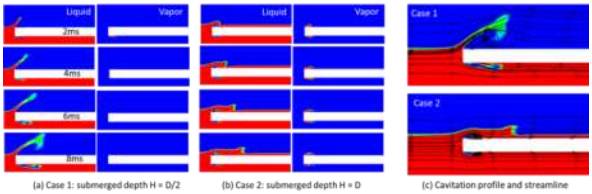

Fig. 4. Detailed cavitation profiles during the growth process in case 1 and case 2.

Fig. 3 shows a comparison of the cavitation growth process between experimental images [5] and numerical simulation at the time of 2, 4, 6, and 8 ms. The growth of the cavitation was well simulated and match the experimental images. The projectile was launched at a velocity of 19.1 ms and creates a cavity that grows from the head of the projectile. The water layer near before the head leaps above the free surface. The cavity continues to grow and is opened to the air. Due to the lower pressure inside the cavity, air moves down and into the cavity, and replaces entire natural cavitation by air entrainment as shown in Figs. 4 (a).

To analyses the effect of submerged depth on the growth of the cavitation profile, a simulation of case 2, in which the flow with a depth $H = D$ and at the same velocity in case 1. Figs. 4 and 5 show comparisons of the simulations of case 1 and case 2. Cross 2D sections with streamlines show the air entrainment into the cavity in case 1, while the cavity is closed in case 2 with natural cavitation. It can see in these, the natural cavity in case 2 grows slowly and due to the re-entry jet as shown in Figs. 5 (b-c), the cavity breaks off in

* Corresponding Author: Van-Tu Nguyen, nguyenvantu@live.com; Warn-Gyu Park, wgpark@pusan.ac.kr

the tail region, while the water leaped above the free surface keeps flow downstream. In case 1, there is no re-entry jet (Fig. 5 (c)) and the air cavity continues growing much larger than the cavity in case 2.

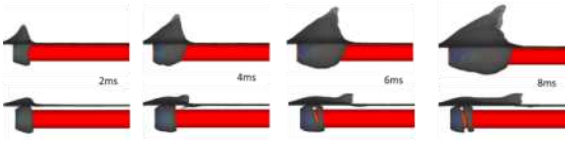

Fig. 5. Evolution of cavitation profile during the growth process in case 1 (top) and case 2 (bottom).

For investigating the effect of velocities on the growth process of the flow, the simulations at velocities of 30 m/s (case 3), 40 m/s (case 4), and 50 m/s (case 5) were performed. Fig. 6 shows both liquid and vapor phases in each case. It is similar to case 1 that the air entrainment causes natural cavitation to vanish, while the natural cavity still grows in the lower side of the projectile in cases 4 and 5.

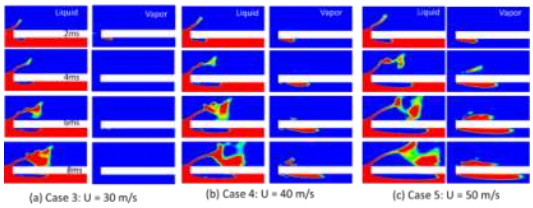

Fig. 6 Evolution of cavitation profiles during the growth process in cases 3-5.

4. Conclusions

This work provides a numerical investigation of supercavitating flow around a high-speed projectile near a free surface. The submerged depth of the projectile and velocity have strong effects on the growth process of the flow. In case of the projectile placed deeper (depth $H = D$), the cavity is closed and a re-entry jet occurs and breaks the cavity, while in case of the projectile coincides with the free surface, the cavity opens to the air and air entrainment occurs. At larger velocities, the cavity closes earlier and the cavity grows and contains both air and vapor.

Acknowledgments: This work was supported by Basic Science Research Program through the National Research Foundation of Korea (NRF) funded by the Ministry of Education (No. 2020R1I1A3067229), and (No. 2020R1I1A1A01072475).

References

[1] Nguyen V-T, Park W-G. Enhancement of Navier–Stokes solver based on an improved volume-of-fluid method for complex interfacial-flow simulations. Appl Ocean Res. 2018;72:92-109.
[2] Nguyen V-T, Phan T-H, Park W-G. Modeling and numerical simulation of ricochet and penetration of water entry bodies using an efficient free surface model. Int J Mech Sci. 2020;182:105726.
[3] Dias F, Ghidaglia J-M. Slamming: Recent Progress in the Evaluation of Impact Pressures. Annu Rev Fluid Mech. 2018;50:243-73.
[4] Wang Y, Xu C, Wu X, Huang C, Wu X. Ventilated cloud cavitating flow around a blunt body close to the free surface. Physical Review Fluids. 2017;2:084303.
[5] Xu C, Huang J, Wang Y, Wu X, Huang C, Wu X. Supercavitating flow around high-speed underwater projectile near free surface induced by air entrainment. AIP Advances. 2018;8:035016.
[6] Nguyen V-T, Vu D-T, Park W-G, Jung C-M. Navier–Stokes solver for water entry bodies with moving Chimera grid method in 6DOF motions. Comput Fluids. 2016;140:19-38.
[7] Phan T-H, Shin J-G, Nguyen V-T, Duy T-N, Park W-G. Numerical analysis of an unsteady natural cavitating flow around an axisymmetric projectile under various free-stream temperature conditions. Int J Heat Mass Tran. 2021;164:120484.

* Corresponding Author: Van-Tu Nguyen, nguyenvantu@live.com; Warn-Gyu Park, wgpark@pusan.ac.kr